Reply to "interactive comments from anonymous Referee #1"

We are particularly grateful to the referee for providing excellent comments and suggestions to significantly improve the manuscript. The crucial concern, regarding the determination of transport times of open crop residue burning (OCRB) plumes and potential influences from sources other than OCRB, is essential to the results of the study. To make the results more robust and representative, we will revise the manuscript according to the referee's comments. It is worth noting that several previous studies have addressed OCRB-dominant pollution episodes at Mount Tai. For example, simulations using the regional transport model demonstrated that over 79% and 80% of EC and OC mass at the summit of Mt. Tai resulted from OCRB emissions (Yamaji et al., 2010). Suthawaree et al. (2010) analyzed the ethane-normalized mixing ratio profiles of NMHCs species and found significant enhancements in the ratios of biomass burning-related species compared to vehicular emission indicators (toluene, *i*-pentane, etc.). Measurements of oxygenated VOCs using PTR-MS also indicated that the ratio Δacetaldehyde/ΔCO increased by a factor of 5 when a site was affected by OCRB plumes (Inomata et al., 2010). In the revised manuscript, we will revisit their major conclusions that support our arguments, which were based on the fact that the influences from sources other than OCRB were small for the episodes studied. As the referee mentioned, there have been a number of studies investigating correlations among carbonaceous aerosols from OCRB or urban sources, but those relating their variations with transport time are scarce. The motivation of this work was to determine the lifetimes of EC and OC from OCRB sources from an observational perspective that assists in process elucidation, improving expressions in chemical transport models.

We have recently undertaken careful sensitivity analyses to estimate uncertainties in transport times, and by extension, uncertainties in the estimated lifetimes. Overall, the major findings of this study were the evident decreases in ΔEC/ΔCO and ΔOC/ΔCO ratios with transport time. The determination of the lifetimes, associated with large uncertainties, was of secondary importance, although the short lifetimes of carbonaceous aerosols from OCRB sources in east China derived in the study could reinforce the view that it is better to use regional-specific parameters for exploring the global budget of carbonaceous aerosols. The detailed replies to the comments of the referee are listed below.

Comment 1*: The transport time of smoke particles was estimated using the FLEXPART_WRF but from which specific plumes as you have got numerous, see the MODIS plot? Is the site influenced by one plume at a time or mixed of many?*

Reply: During the field campaign, the observations at the summit of Mt.Tai were impacted by hybrid OCRB plumes from a number of OCRB fire spots. However, the influential locations were concentrated in a limited area, making the estimated transport time well-constrained.

Geographical locations of the OCRB events in the CEC, determined by MODIS onboard Terra and Aqua satellites, are shown in Auxiliary Figure 1a. As a demonstration, we divided the areas where burning events occurred into five different regions (A: 33–34°N, 112–114°E; B: 33–34°N, 114–116°E; C: 32–35°N, 118–121°E; D: 34–35°N, 116–118°E; S: 33–34°N, 116–118°E). Note that S is the region we used in the original manuscript. As shown, OCRB events were largely concentrated in the S region, although hotspots were also found in other areas of CEC. In the present study, potential source regions of OCRB plumes with respect to the observations at the summit of Mt.Tai (Auxiliary Figure 1c) were estimated by multiplying OCRB emission fluxes (in units of kg/s) in each grid cell by the corresponding source-receptor-relationship (SRR as in Auxiliary Figure 1b, in units of s/kg). Here, OCRB emission fluxes were assumed to be proportional to the number of hotspots detected by MODIS (Auxiliary Figure 1a) in the target grid. SRR, calculated using the FLEXPART_WRF model, was proportional to the particle residence time in a particular grid cell. The estimated potential OCRB source region (Auxiliary Figure 1c) was concentrated in region S (75.3% contribution) based on observations at the summit of Mt.Tai, significantly higher than those from other regions (A (1.6%), B (10.6%), C (4.6%) and D (7.7%)). A sensitivity test of SRR employing different height criteria (< 500 m above the ground, instead of <100 m) in the base case also resulted in a similar contribution (74.4%) from region S.

The transport time uncertainties were also re-estimated by comparing results from the following scenarios: (Scenario 1) Releasing particles from region S homogeneously in time and space (as a base case in the previous manuscript). (Scenario 2) Temporal variations in emissions were accounted for in the number of hotspots detected by MODIS. Data gaps due to the overpass of satellites were filled using linear interpolations. (Scenarios 3–6) Region S was divided into four smaller sub-regions (S1: 33–34°N, 116–117°E; S2: 33–34°N, 117–118°E; S3: 33.5–34°N, 116–118°E; S4: 33–33.5°N, 116–118°E) and the particles were released only from one of the sub-regions at a time. As shown in Auxiliary Figure 2a, a good correlation (intercept = –0.2 h, slope = 1.1, r = 0.93) was obtained for scenarios 1 and 2, indicating that temporal variations in the emission strengths of OCRB had limited impact (variability ~10%) on the estimation of plume transport times. Estimated transport times of plumes from the sub-regions (S1, S2, S3 and S4) were approximately the same as those from region S (Auxiliary Figure 2b), with slopes ranging from 0.89–0.99 and intercepts ranging from 0.7–1.4 h, implying that the estimated transport time was almost independent of the area settings. Correlations among the transport times estimated for sub-regions S1, S2, S3 and S4 demonstrated that the maximum uncertainty related with the OCRB source regions was ~14% (Auxiliary Figures 2c and 2d), and there was approximately a 4h time lag (intercept of best linear fitting). These variations only slightly modified the estimated lifetimes and did not change the main conclusions of this paper (Auxiliary Figure 3).

***Comment 2**: How to attribute ratios of ECa/CO, OC/CO, OC/ECa at transport time (t=0) and becoming the representative of fresh burning plume without suffering any scavenging.*

Reply: The ratios (ΔEC/ΔCO: 15.5 ng/m^3/ppbv, ΔOC/ΔCO: 97.7 ng/m^3/ppbv, ΔOC/ΔEC: 9.8) we showed in the previous manuscript, associated with the lowest transport time, were not at t = 0, but were at t = 0.7 h. They were measured during another field campaign in Rudong, China. The age of the OCRB plumes (0.7 h) was estimated according to the maximum distance (~10 km) between fire spots and the measurement site and the wind speed in the corresponding direction. Detailed descriptions of the characteristics of carbonaceous aerosols during the Rudong field campaign are provided in a separate manuscript (Emission ratio of carbonaceous aerosols observed near crop residual burning sources in a rural area of the Yangtze River Delta Region, China, under minor revision in JGR, 2012). As highlighted by the referee, accurate determinations of the ratios of ΔEC/ΔCO and ΔOC/ΔCO for fresh OCRB plumes are essential for estimations of their lifetimes. Based on the comment of the reviewer, we carefully re-examined the Rudong data and decided to exclude them based on the following considerations: (1) Chemico-physical properties of the carbonaceous aerosols may differ between the field campaigns at Mt.Tai in 2006 and in Rudong in 2010 because a large quantity of rape plant residues were also burned near Rudong in addition to wheat residues. (2) The method of estimating the age of OCRB plume in Rudong was quite different from that at Mt.Tai and combining these two case studies introduced large uncertainties. (3) As mentioned in the text, EC and OC mass concentrations measured for the Mt.Tai campaign were from PM_1, different from those (from $PM_{2.5}$) during the Rudong campaign. Inclusion of data from Rudong could overestimate the ΔOC/ΔCO ratios substantially for fresh OCRB plumes, because OC is also present in larger particles. The revised analysis demonstrated that the estimated lifetime of EC (4.2 days) was generally unchanged from the previous result (4.3 days). However, the estimated lifetime of OC (1.8 days) increased by 50%. Furthermore, the lifetimes of EC and OC were estimated under six different scenarios (described in the reply to comment 1) to estimate their uncertainties. Results demonstrated that the lifetime of EC ranged from 98.4–136.9 h (4.1–5.7 days), which was comparable with previous estimates. ΔEC/ΔCO ratios at the transport time t = 0 (y-intercept of fitting curve) ranged from 15.0–16.6 ng/m^3/ppbv, slightly higher than measurements from fresh biomass burning plumes (9.4 ng/m^3/ppbv, Andreae and Merlet (2001); 13.8 ng/m^3/ppbv, Schwarz et al., (2008); 11.1 ng/m^3/ppbv, Spackman et al., (2008)). The lifetime of OC was found to be 28.0–44.2 h (1.2–1.8 days). ΔOC/ΔCO ratios at the transport time t = 0 ranged from 58.8–65.5 ng/m^3/ppbv. To quantitively study the dependence of ΔOC/ΔEC ratios on transport time, linear regressions were used in the revised manuscript instead of exponential decay fittings in the previous manuscript. We found that the ΔOC/ΔEC ratio of OCRB plumes decreased gradually with increasing transport time (slopes ranging from –0.06– to –0.03 h^{-1}), indicating that the removal of OC from the atmosphere is more efficient than that of EC. Scatter plots of relationships among carbonaceous aerosol correlations and transport time with fitting

results are shown in Auxiliary Figure 3 (Scenario 1 and 2) and Auxiliary Figure 4 (Scenarios 3, 4, 5, 6).

Comment 3*: I am not sure if the ratios of ΔEC/ΔCO and ΔOC/ΔCO can be fixed for various plumes (presumably if they are in different stages (flaming/smoldering) of biomass burning surrounding the site)*

Reply: We agree with the referee's opinion that variations in the carbonaceous aerosol correlations (ΔEC/ΔCO, ΔOC/ΔCO) from OCRB would depend on the phase of combustion. Flaming combustion tends to oxidize carbonaceous material to the final oxidation product (CO_2) at high temperatures, leading to lower $\Delta CO/\Delta CO_2$ ratios. Smoldering, however, would produce more CO resulting from incomplete combustion. To improve representativeness, we used CO-CO_2 correlations to illustrate the completeness of OCRB combustion. As shown in Auxiliary Figure 5, data points for these two cases showed little scatter and linear regressions of the CO-CO_2 scatter plots demonstrated that the slopes for the two cases were similar, with ratios of 42.3 ppbv/ppmv (r = 0.97) and 40.2 ppbv/ppmv (r = 0.90) for the OCRB episodes on June 6–7 and June 12–13, respectively. The results were between the values for flaming combustion (4.2 ppbv/ppmv) and smoldering combustion (69.9 ppbv/ppmv) of OCRB reported for the Rudong campaign, indicating that the OCRB plumes observed at Mt.Tai were likely to be smoldering-dominated. The similar burning conditions in the source region for these two cases could justify combination analysis of the two discrete cases to investigate the lifetime of carbonaceous aerosols, without being affected by the combustion stage of biomass burning.

Comment 4*: In China fossil fuel based emissions are also significant sources of carbonaceous species, and how to delineate the influence is not described?*

Reply: As suggested by the referee, mixing with outflowed urban pollution could alter the carbonaceous aerosol correlations of OCRB plumes measured at the receptor site, resulting in large uncertainties in estimating their lifetime. However, the influence of fossil fuels was relatively small in the two studied cases. During high-pollution episodes from June 5–7 and June 12–13, OCRB emissions in CEC were responsible for 79 and 80% of BC and OC mass concentrations measured at the summit of Mt. Tai based on calculations using the Community Multi-scale Air Quality Modeling System (shown in Auxiliary Figure 6). Also, the contributions from OCRB sources ranged from 65–87% (BC) and from 64–93% (OC) for the targeted episodes in this study. Variations in carbonaceous aerosol mass concentrations during urban air pollution-dominated periods (after June 15) were well-captured by the simulations, implying that uncertainties in the urban emissions inventory (REASv1.0, Ohara et al., 2007) had a very limited impact on simulations in the OCRB-dominant case. We also simulated the mass concentrations of carbonaceous aerosols based on a bottom-up emissions inventory (INTEX-B 2006, Zhang et al., 2009) and a source-receptor-relationship (SRR) determined using the FLEXPART_WRF

model. Detailed descriptions of the calculation of the SRR using backward simulations have been published (Stohl et al., 2009). Simulations assumed that transported particles did not suffer any loss from dry deposition and cloud scavenging. Even so, approximately 78% of the BC mass measured at the site could not be explained by anthropogenic emissions (industry, transport, domestic heating and power plants). We attributed that mass to OCRB sources. This result was generally consistent with the simulations using CMAQ models. The ratios of ΔEC/ΔCO and ΔOC/ΔCO for OCRB plumes can be quantitatively estimated assuming that the carbonaceous aerosol correlations measured at the site were weighted linear combinations of urban and OCRB pollution (equation: $\frac{\Delta[x]}{\Delta CO}\Big|_{obs} = f_{urban}\frac{\Delta[x]}{\Delta CO}\Big|_{urban} + f_{OCRB}\frac{\Delta[x]}{\Delta CO}\Big|_{OCRB}$, where f represents the respective contribution and x refers to EC or OC. We assumed that the ΔEC/ΔCO and ΔOC/ΔCO ratios for urban pollution did not change significantly over 2 days). The ratios of ΔEC/ΔCO (6.5 ng/m^3/ppbv, Pan et al., 2011) and ΔOC/ΔCO (23.5 ng/m^3/ppbv) for urban pollution in CEC were adopted. The results demonstrated that the ΔEC/ΔCO and ΔOC/ΔCO ratios were 12 and 23% higher, respectively, than the observations. Applying the revised ratios to the calculation, we found that the lifetimes of EC and OC were generally consistent with the previous results, with means of 111.5 h (4.6 days) for EC and 25.8 h (1.1 days) for OC. Large variabilities in ΔEC/ΔCO and ΔOC/ΔCO ratios have been reported for urban pollution because of diverse emission sources in different locations. To justify the results, we performed sensitivity tests using different ΔEC/ΔCO ratios (4.8 ng/m^3/ppbv in Beijing, reported by Han et al., (2009); 9.8 ng/m^3/ppbv in Bangkok, reported by Sahu et al., (2011)) and ΔOC/ΔCO ratios (14–84 ng/m^3/ppbv, reported by Maria et al.,(2003)) of urban pollution. We found that the estimated lifetimes of EC and OC had less than 10% variance, even if ΔEC/ΔCO and ΔOC/ΔCO ratios for urban pollution changed by a factor of 2. This suggests that the influence of urban pollution was limited. In the revised manuscript, we will follow the referee's suggestion to add corresponding contents and describe the potential impact of non-OCRB sources.

Comment 5*: the measurements period is too short just several days in the month of June 2006. Analysis should be represented by reasonably LONG PERIOD of observations.*

Reply: It is a good suggestion to perform longer time-periods of observations of OCRB pollution. OCRB activities in China occur in short periods, on different days, each year depending on the time of harvest. There are normally several days when crop residues are intensively burned. Statistical analyses on hotspot data (2006–2008) obtained from a MODIS satellite indicated that over 85% of fire events occurred in June (harvest season in CEC). In this study, we endeavored to find episodes with maximum representativeness. Biomass burning in June was estimated to be responsible for 40% of the annual OCRB emissions in 2006 and emissions on June 7 accounted for 14% of the total OCRB emissions in June. In the future, we will follow the referee's suggestion. We are currently continuing observations on variations in carbonaceous aerosols from OCRB in China.

Comment 6*: Schemes of FLEXPART WRF model and definition of transport time should be separately presented in a subsection before discussing the observations.*

Reply: Schemes of FLEXPART have been explicitly described by Stohl et al., (2009) and the incorporation of FLEXPART with WRF has been presented in their technical notes. In the manuscript, we described the simulation settings in Section 2.2. We will follow the referee's advice to briefly introduce the FLEXPART schemes separately.

Comment 7*: Measurements of BCe in PM1 and PM2.5 were done alternatively in time reference; therefore samples are different for PM1 and PM2.5. Then what is the use of such correlation if BCe is not measured simultaneously, I mean how you adjusted the time lag.*

Reply: We agree with the referee's arguments that the mass concentration measurements of BC_e in PM_1 and $PM_{2.5}$ by automatically altering the cyclone cut-offs (every 30 min) might introduce uncertainties, since the chemo-physical properties of particles are not necessarily identical for the cycle and the bias from the time lag can be significant if the measurements are made in the proximity of sporadic BC sources. For example, emissions of BC from on-road vehicles vary over several orders of magnitude under different traffic conditions. However, this influence is small when measurements are made far away from the source regions, as was the case in this study. A previous study (Kanaya et al., 2008) showed excellent correlation (slope: 0.92, r^2 = 0.91) between BC_PM_1 and BC_$PM_{2.5}$, since temporal variations in BC mass concentrations were dominated by low-frequency components. We suggest that the measurements in this study were reasonable to use.

References:

Fu, P., K. Kawamura, K. Okuzawa, S. G. Aggarwal, G. Wang, Y. Kanaya, and Z. Wang, Organic molecular compositions and temporal variations of summertime mountain aerosols over Mt. Tai, North China Plain, J. Geophys. Res, 113, D19107, 2008.

Han, S., Y. Kondo, N. Oshima, N. Takegawa, Y. Miyazaki, M. Hu, P. Lin, Z. Deng, Y. Zhao, N. Sugimoto, and Y. Wu (2009), Temporal variations of elemental carbon in Beijing, J. Geophys. Res., 114(D23), 10.1029/2009jd012027.

Inomata, S., H. Tanimoto, S. Kato, J. Suthawaree, Y. Kanaya, P. Pochanart, Y. Liu, and Z. Wang, PTR-MS measurements of non-methane volatile organic compounds during an intensive field campaign at the summit of Mount Tai, China, in June 2006, Atmospheric Chemistry and Physics Discussions, 9(6), 26697-26734, 2009.

Kanaya, Y., Y. Komazaki, P. Pochanart, Y. Liu, H. Akimoto, J. Gao, T. Wang, and Z. Wang, Mass concentrations of black carbon measured by four instruments in the middle of Central East China in June 2006, Atmos Chem Phys, 8(24), 7637-7649, 2008.

Kondo, Y., Y. Komazaki, Y. Miyazaki, N. Moteki, N. Takegawa, D. Kodama, S. Deguchi, M. Nogami, M. Fukuda, and T. Miyakawa (2006), Temporal variations of elemental carbon in Tokyo, J. Geophys. Res, 111, 10.1029/2005JD006257.

Ohara, T., Akimoto, H., Kurokawa, J., Horii, N., Yamaji, K., Yan, X., and Hayasaka, T.: An Asian emission inventory of anthropogenic emission sources for the period 1980–2020, Atmos. Chem. Phys., 7, 4419-4444, doi:10.5194/acp-7-4419-2007, 2007.

Pan, X. L., Y. Kanaya, Z. F. Wang, Y. Liu, P. Pochanart, H. Akimoto, Y. L. Sun, H. B. Dong, J. Li, H. Irie, and M. Takigawa (2011), Correlation of black carbon aerosol and carbon monoxide in the high-altitude environment of Mt. Huang in Eastern China, Atmos. Chem. Phys., 11(18), 9735-9747, 10.5194/acp-11-9735-2011.

Sahu, L. K., Y. Kondo, Y. Miyazaki, P. Pongkiatkul, and N. T. Kim Oanh (2011), Seasonal and diurnal variations of black carbon and organic carbon aerosols in Bangkok, J. Geophys. Res., 116(D15), D15302, 10.1029/2010jd015563.

Schwarz, J. P., R. S. Gao, J. R. Spackman, L. A. Watts, D. S. Thomson, D. W. Fahey, T. B. Ryerson, J. Peischl, J. S. Holloway, M. Trainer, G. J. Frost, T. Baynard, D. A. Lack, J. A. de Gouw, C. Warneke, and L. A. Del Negro (2008), Measurement of the mixing state, mass, and optical size of individual black carbon particles in urban and biomass burning emissions, Geophys. Res. Lett., 35(13), L13810, 10.1029/2008gl033968.

Spackman, J. R., J. P. Schwarz, R. S. Gao, L. A. Watts, D. S. Thomson, D. W. Fahey, J. S. Holloway, J. A. de Gouw, M. Trainer, and T. B. Ryerson (2008), Empirical correlations between black carbon aerosol and carbon monoxide in the lower and middle troposphere, Geophys. Res. Lett., 35, L19816, doi:10.1029/2008GL035237.

Stohl, A., et al. An analytical inversion method for determining regional and global emissions of greenhouse gases: Sensitivity studies and application to halocarbons, Atmos. Chem. Phys., 9, 1597-1620, 2009.

Suthawaree, J., S. Kato, K. Okuzawa, Y. Kanaya, P. Pochanart, H. Akimoto, Z. Wang, and Y. Kajii, Measurements of volatile organic compounds in the middle of Central East China during Mount Tai Experiment 2006(MTX 2006): observation of regional background and impact of biomass burning, Atmos Chem Phys, 10(3), 1269-1285, 2010.

Yamaji, K., J. Li, I. Uno, Y. Kanaya, H. Irie, M. Takigawa, Y. Komazaki, P. Pochanart, Y. Liu, H. Tanimoto, T. Ohara, X. Yan, Z. Wang, and H. Akimoto, Impact of open crop residual burning on air quality over Central Eastern China during the Mount Tai Experiment 2006 (MTX2006), Atmos. Chem. Phys., 10(15), 7353-7368, 10.5194/acp-10-7353-2010, 2010.

Zhang, Q., Streets, et al., Asian emissions in 2006 for the NASA INTEX-B mission, Atmos. Chem. Phys., 9, 5131-5153, doi:10.5194/acp-9-5131-2009, 2009.

Auxiliary Figures:

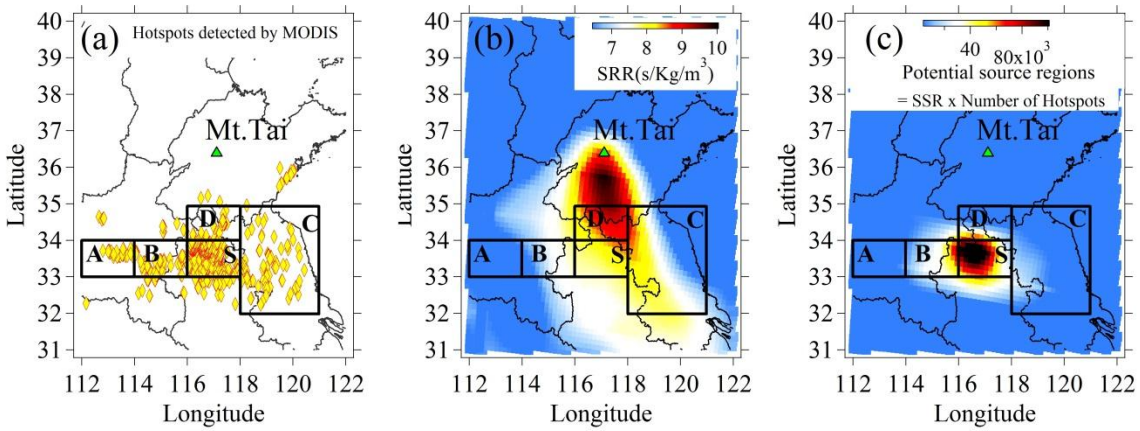

Auxiliary Figure 1. (a) Spatial distribution of hotspots detected by MODIS. (b) Source-receptor-relationship in a footprint region calculated by backward simulation of the FLEXPART_WRF model. (c) Potential source region (in arbitrary units) of OCRB plumes observed at the summit of Mt.Tai.

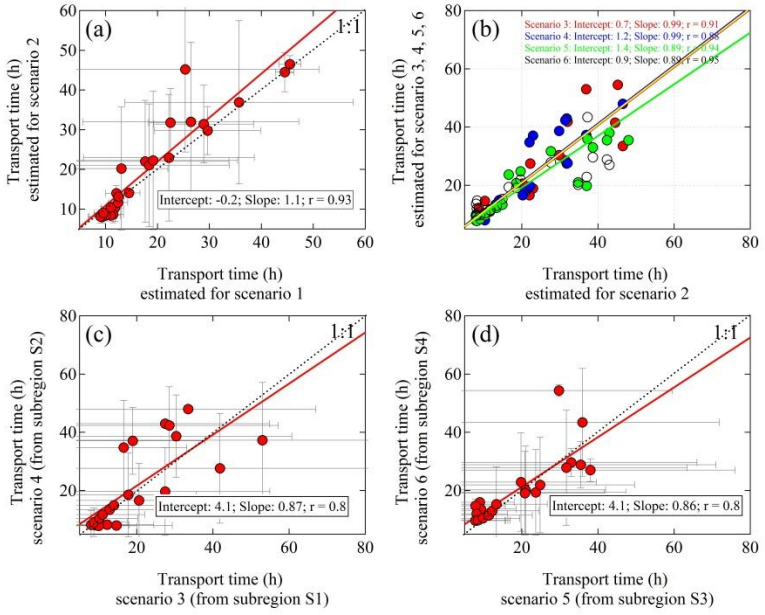

Auxiliary Figure 2. Scatterplots and their linear regressions for transport times under different emission scenarios.

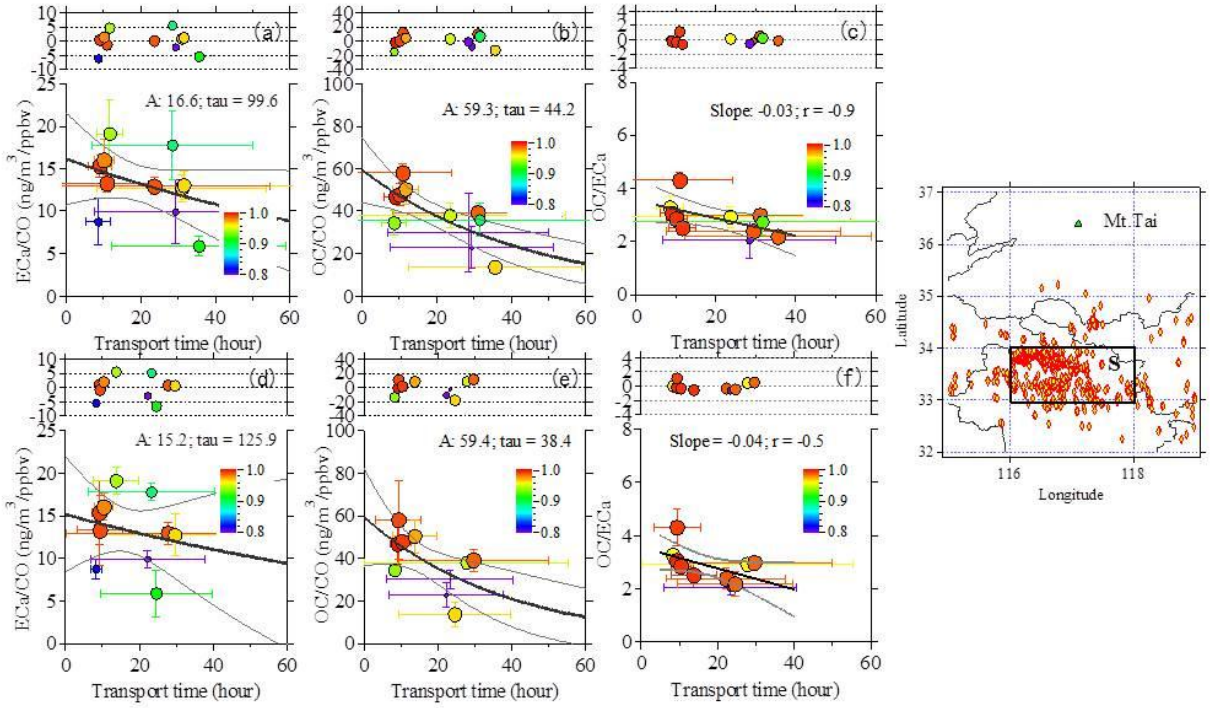

Auxiliary Figure 3. Fitting results for the relationships between variations in ΔEC/ΔCO, ΔOC/ΔCO and ΔOC/ΔEC ratios and transport time for scenarios 1(a–c) and scenarios 2(d–f). The gray lines in the figure represent the 90% confidence intervals.

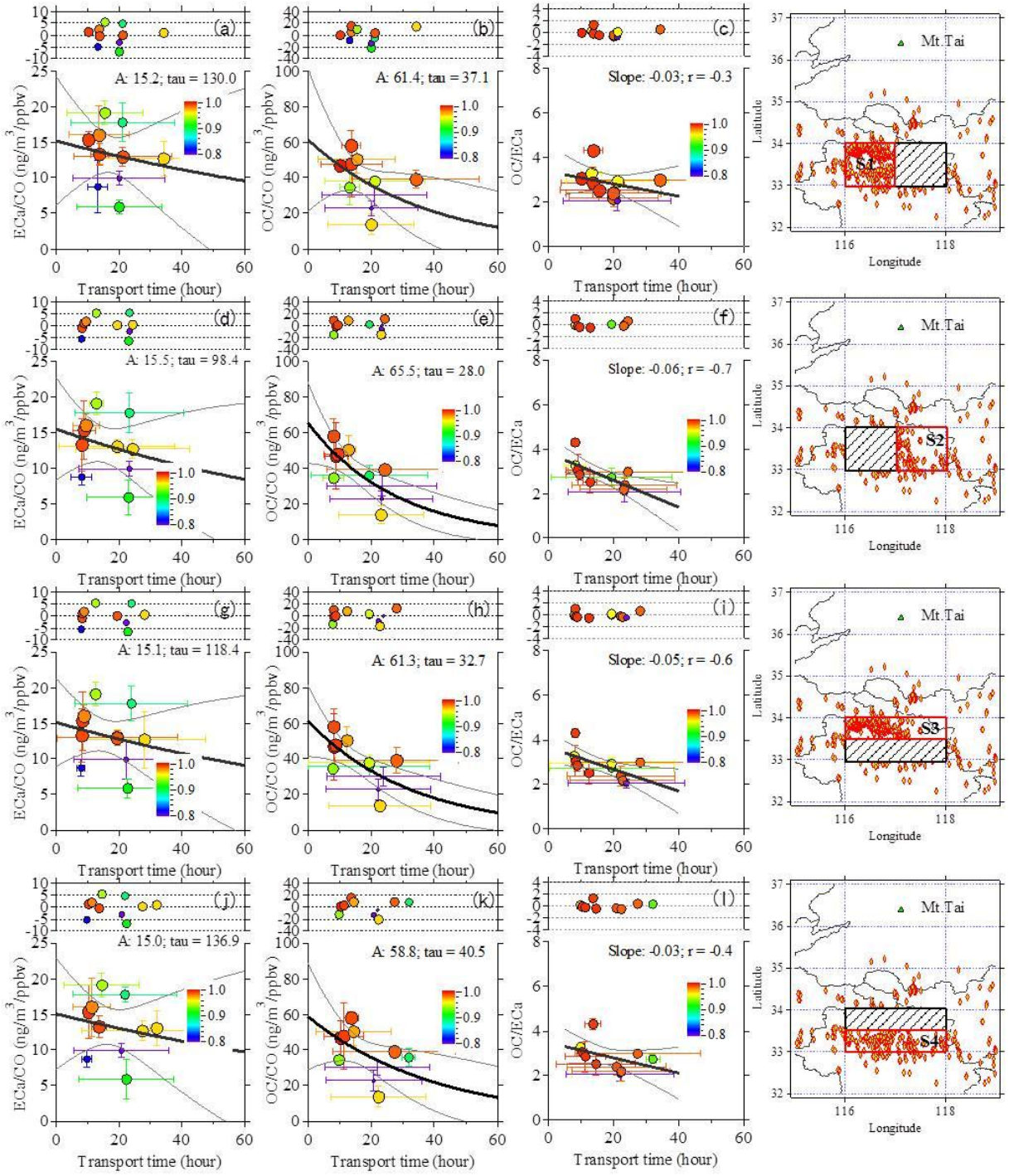

Auxiliary Figure 4. Fitting results for the relationships between variations in ΔEC/ΔCO, ΔOC/ΔCO and ΔOC/ΔEC ratios and transport time for scenarios 3(a–c), scenarios 4(d–f), scenarios 5 (g–i) and scenarios 6 (j–l). Four figures in the rightmost panel indicate the source regions where tracer particles were released by the FLEXPART_WRF model. The gray lines in the figure represent the 90% confidence intervals.

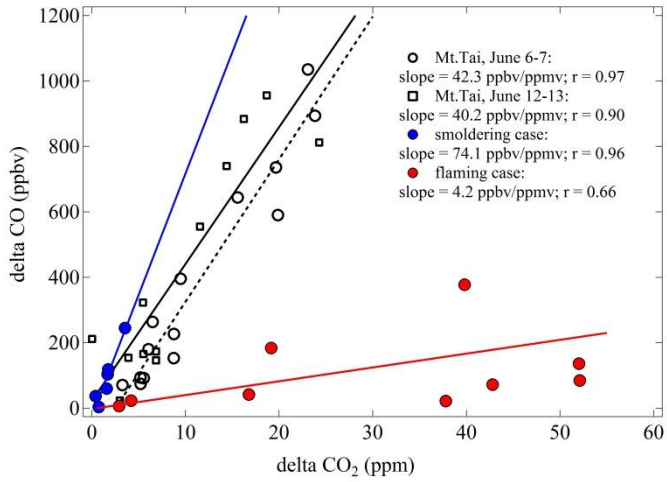

Auxiliary Figure 5. CO-CO_2 correlations for OCRB-dominant cases from June 6–7 (circles) and June 12–13 (squares). For comparison, we includes the flaming (red dots) and smoldering (blue dots) combustion cases observed in the proximity of burning sources during an intensive OCRB burning period in 2010 at Rudong.

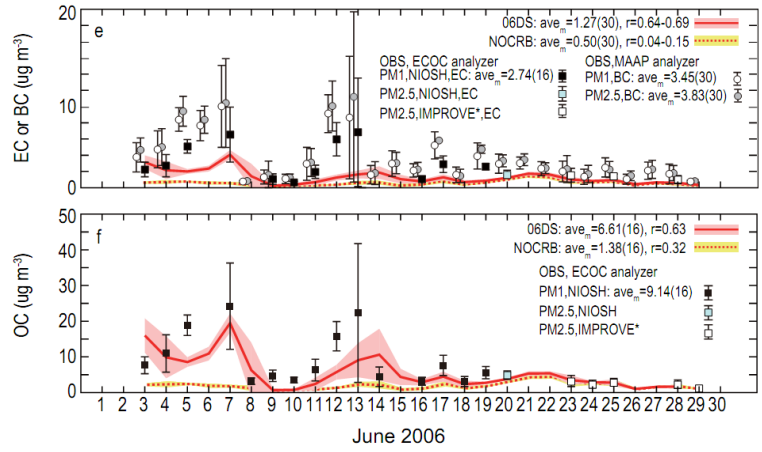

Auxiliary Figure 6. Simulated mass concentrations of carbonaceous aerosols during the field campaign. This plot was published by Yamaji et al., 2010.